

DETECTION AND MAPPING OF THE DISASTER-STRICKEN AREAS FROM LANDSAT DATA

Shinkichi Kishi and Hiroshi Ohkura
National Research Center for Disaster Prevention,
Science and Technology Agency
3-1 Tennodai, Tsukuba-city, Ibaraki-ken
Japan
VII

ABSTRACT

Disaster-stricken areas in Japan due to natural disasters have been promptly detected from LANDSAT MSS and TM data. Detected areas were mapped in pixel-wise directly onto the published topographic map by the plotter with color-pens. Images were projected onto the UTM coordinates using ground control points and affine transformation and detection of the area was conducted based on the spectral characteristics changed before and after the disaster. Through the study it was found that mapping of the locations of landslides in mountainous region from TM data was effective in comparison with tentative manual mapping from aerial photographs and that the resolution and the spectral bands of TM data were practical in the case of disaster caused by flood or volcanic eruption.

INTRODUCTION

Advantages of the information acquired by satellite remote sensing are in simultaneity of wide area, periodicity, computer compatibility and spectral characteristics, and especially in the easiness to compare the data before and after the disaster.

Since the start of receiving of LANDSAT data in Japan in 1979, application studies of remote sensing technology have been promoted in the field of disaster prevention, centering around the detection of the areas stricken by the remarkable natural disasters which occurred in Japan frequently in the period.

In the beginning chapters the digital techniques for detection and mapping of disaster-stricken areas from LANDSAT MSS and TM data are described and in the following chapters the examples applied to each disaster caused by flood, landslide and volcanic eruption are presented.

1. SPECTRAL CHARACTERISTICS OF DISASTROUS PHENOMENA

In remote sensing, based upon the spectral characteristics, an object or an objective area is considered to be composed of three fundamental elements, namely, inorganic substances, vegetation and water. Spectral signature of inorganic substance presents a peak in visible region and that of vegetation presents a peak in near-infrared region. Radiance of water is feeble in both regions.

As for the scale of radiance of object, usually the digital values recorded in CCT(Computer Compatible Tape) processed by the receiving station are used because of the difficulties in conversion into physical values of radiance.

For the method of detection of disaster-stricken areas from the satellite data, it is effective to compare the images at the two times before and after the disaster as close as possible in the similar season and to detect the change of land covering in the lapse of the two times. In many cases of natural disasters appropriate for satellite remote sensing the stricken areas are mainly in fields and mountains covered by vegetation. Aspect of the variation of spectral characteristics of land covering depends on the kind of disastrous phenomena.

2. PROCEDURE OF DETECTION OF DISASTER-STRICKEN AREAS

2.1 Geographic correction into the topographic map

Flow chart of data processing is shown in Fig. 1. In the first step the image data in CCT are rearranged onto the UTM coordinates system of the published topographic map by the geographic correction using GCP (Ground Control Point) and affine transformation.

2.2 Radiometric correction between the two times

In order to compare the images at the two times before and after the disaster the radiometric correction for each band is conducted based upon the linear regression analysis relatively between the two times. Here, indicating training areas where the change of land covering in the lapse of the two times is considered to be small, usually the data before disaster are corrected. In this step, for a scale of evaluating the significant value of the difference of the data at the two times, standard deviation of difference in the training areas is calculated.

2.3 Difference/Ratio image of the data at the two times

Using the difference image for each band made by subtracting the data at the two times from each other in which the geographic and radiometric correction were performed, extraction of the changed parts of land covering is conducted in parallel with examination of the spectral characteristics at representative spots. As in the case of mountainous area some localities in the level of radiance attributable to the relation between the topography and the sun direction are seen in the image, the ratio made by dividing the data at the two times is used.

2.4 Supervised classification of the image after disaster

In such a case of lacking suitable data before disaster or of considering the characteristics

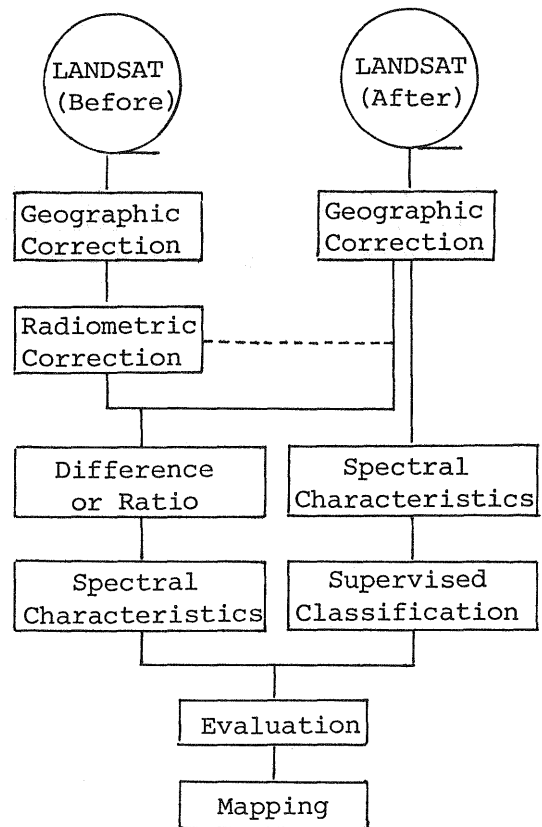


Fig. 1 Data processing

of the disaster, detection of the stricken areas is conducted by the maximum likelihood method or the level-slicing with the data after disaster alone.

2.5 Data transmission of earth observation image

Recently the experiments of the data transmission of LANDSAT and MOS1 image from EOC (Earth Observation Center) of Japan to our Center via the public transmission line were successfully conducted in the personal microcomputer level with floppy disk. LANDSAT TM data of Izu-Ohshima island stated in Chapter 6 were acquired in this way.

3. MAPPING TECHNIQUE OF LANDSAT DATA

The result of detection of the stricken areas is not practical until its positional correspondance to the published topographic map is clarified. Therefore it is effective to plot the result directly onto the map or onto it's copy or onto the tracing paper which can be overlaid on the map.

The direct mapping onto the map is performed as follows. Inputting the XY coordinates of the four corner of the map set on the plotter using the digitizing sight, then the position on the map of the pixel in the image file is determined by the XY coordinates calculated in the following formula.

$$x = [j \{ix_3 + (m-i)x_4\} + (n-j) \{ix_2 + (m-i)x_1\}] / mn$$

$$y = [j \{iy_3 + (m-i)y_4\} + (n-j) \{iy_2 + (m-i)y_1\}] / mn$$

The formula is derived from the consideration that the map coordinates (x,y) is the projection of the image coordinates (i,j) of the pixel which should be divide the opposite side of the map in proportional distribution in the similar direction as is shown in Fig. 2.

For another method of mapping, giving the coordinates in longitude and latitude corresponding to the four corner of the image corrected geographically beforehand, mapping onto the free paper such as tracing paper is possible based upon the UTM coordinates system.

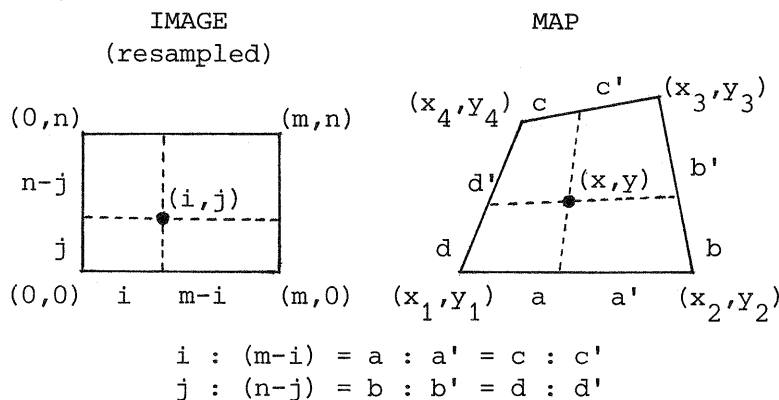


Fig. 2 Simple projection between image and map

4. DETECTION OF THE REGIONAL DISTRIBUTION OF THE DAMAGE ON RICE-PLANT DUE TO THE FLOOD

In August 1986, Kashimadai-town located in the north-east district of Japan was stricken by the severe flood caused by the heavy rain stimulated by the approaching typhoon. Slicing the CCT-count of LANDSAT TM band 4 taken a month after the flood, the regional distribution of the degree of the damage on rice-plant in harvest season was detected and was found to coincided well with the data of yield surveyed by the town office.

4.1 LANDSAT TM data and geographic correction

Low cloudiness and useful data was of a year before and of a month after the flood. Based on the affine transformation with about ten GCPs and the nearest neighborhood resampling they were geographically projected to the 1:25,000 topographic map of the UTM system. Mesh size of resampling was set to 1.171875" in latitude and 0.9375" in longitude. This mesh size is almost regular square of about 28.5 x 28.5 meters at the latitude of the study area (38°30'N) and equivalent to the size of original pixel. As for the geographically corrected image of a month after the flood, Band 3 of visible region and Band 4 of near-infrared region is shown in Photo 1 and Photo 2 respectively.

4.2 Level-slicing of the value of Band 4

Vitality of vegetation like rice-plant is considered to be reflected sensitively on the value observed in Band 4 of near-infrared region. Half tone picture of slicing the CCT-count in the equal interval of 10 is shown in Photo 3. Assigned densities to each classified area is shown on the right hand in the photo, in such a way the heavier the damage the darker the tone. Here the paddy fields were extracted from the image a year before the flood by the supervised classification.

On the other hand, in order to back up the evaluation of the damage on rice-plant in each classified region, spectral characteristics of representstive spots selected in each region were examined. Sampling areas are shown in Photo 2 and the spectral signatures are shown in Fig. 3 with the area numbers.

Further, Fig. 4 shows the map plotted the same contents as in Photo 3. Here, setting the interval of slicing to 20 in CCT-count, the study area was divided into four regions from the limitation of the kinds of distinguishable symbols.

4.3 Comparison with the ground survey data

From the linear regression analysis between CCT-count of Band 4 and the yield examined by the town office by sampling actual rice-plant, the following formula was obtained.

$$Y = 0.093 X - 5.165$$

where X denotes CCT-count and Y denotes the yield(kg/10a). The correlation coefficient resulted in 0.86. According to the formula the slicing value could be expressed in the scale of the yield. Table 1 shows the correspondance among the data of slicing level of CCT-count, length of the period of inundation and yield.

4.4 Regional distribution of the damage on rice-plant

From the above mentioned photos and figures it could be roughly judged that the regions of CCT-counts less than 99 were the paddy fields affected more or less from the flood. Especially the paddy fields in the regions of number 1 and 2 are guessed as the state of dried up swamp from the reason that the radiance of visible band is large and that of near-infrared band is small and in addition that of Band 5 in middle-infrared region is also high.

The topography of the study area is characterized of the large swamp in the past in the central part and becomes gradually higher toward the environs. The regional distribution of the damage of rice-plant detected from LANDSAT TM data a month after the flood well coincided with the length of the period of inundation and with the actual yield, reflecting honestly the topographic condition. These results were highly evaluated and especially the distribution map plotted with 8 color-pens was practically used by the local administrative organ.

5. DETECTION OF LANDSLIDES IN THE MOUNTAINOUS AREA

In September 1984, Ohtaki-village in the mountainous area in the central part of the main land of Japan was attacked by the great landslides caused by the earthquake of magnitude 6.8.

5.1 Detection from LANDSAT MSS data before and after the disaster

An analysis for the purpose of grasping rapidly the whole view of the disaster was conducted from MSS data received and processed by EOC. The first chance of acquisition of low cloudiness data was in nine days after the disaster. For the data before the disaster the one in May 1984 was available.

In the difference image of the two times the landslides were interpreted as the changed parts of land covering mainly from forest to soil. Here, in the image, the root area of the largest landslide was regrettably under the clouds.

5.2 Detection from LANDSAT TM data taken in the next summer

Although, in October 1984, about a month after the disaster TM data was acquired, it was very cloudy. Since that time, after the lapse of snow-covered winter season, cloudless TM data of good quality was acquired for the first time in July 1985 about ten months after the disaster. It caught the whole view of the landslides. The image of Band 3 and Band 4 is shown in Photo 4 and in Photo 5 respectively.

From the data landslides were classified as a category of land covered by soil through the maximum likelihood method. Fig. 5 shows the boundaries of landslides detected from TM data. Fig. 6 shows the boundaries of landslides mapped by hand from aerial photographs and digitized.

Overlaying these figures it was found that landslide on the sunshine slope covered by vegetation is able to be detected with minor axis more than 10 meters and that delicate slippages

in the location of landslide were seen at places. Then mapping the locations directly onto the topographic map it was found that the slippages were seen in the particular case of the area lacking convenient target in manual mapping such as a wood-land path and therefore it could be said that the mapping accuracy of the location of landslide in a target-less forest was higher in using TM data.

6. DETECTION OF THE AREAS COVERED BY VOLCANIC EJECTA DUE TO ERUPTION

In November 1986, Izu-Oshima, one of active volcanoes in Japan, located in the ocean about 100km south of Tokyo historically erupted. The areas covered by lava and volcanic ash were detected from LANDSAT TM data before and after the eruption, taken in January 1985 and in December 1986 respectively.

Volcanic ejecta are inorganic substances and then if they cover the vegetation area radiance in visible region increases and in near-infrared region decreases. Then, outputting the ratio images of Band 3,4 and 5, it was found that detection of the change of land covering is easily conducted in Band 4.

Pixels signifying larger variation of radiance were plotted in the map in Fig. 7 in such a way the smaller the ratio the darker the symbol. The dark plotted parts correspond to the area covered by lava or large scale ejecta and light plotted parts correspond to the area covered by the volcanic ash.

CONCLUSIONS

- 1) The mapping technique developed in the study using the XY plotter with digitizing sight and color-pens is unique and very effective for the practical use of LANDSAT data.
- 2) In the case of mapping of the location of landslide in target-less area the mapping from LANDSAT data is more effective and more accurate than the tentative manual mapping from aerial photographs.
- 3) Resolution and spectral bands of LANDSAT TM data are practical in detection and mapping of the distribution of the regions stricken by flood or by volcanic eruption.
- 4) To realize the administrative use in disaster prevention of orbital satellite remote sensing it is indispensable to increase the frequency of observation.

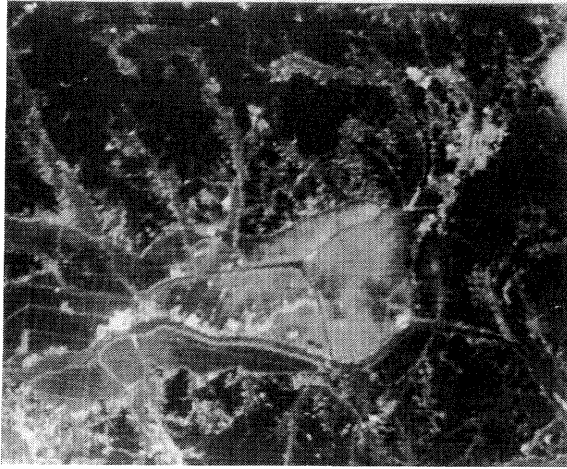


Photo 1
TM image of Band 3
of the damaged
paddy field

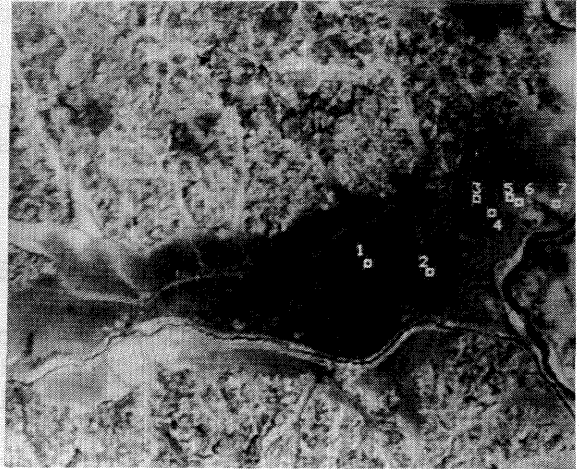


Photo 2
TM image of Band 4
with sampling areas
for spectra

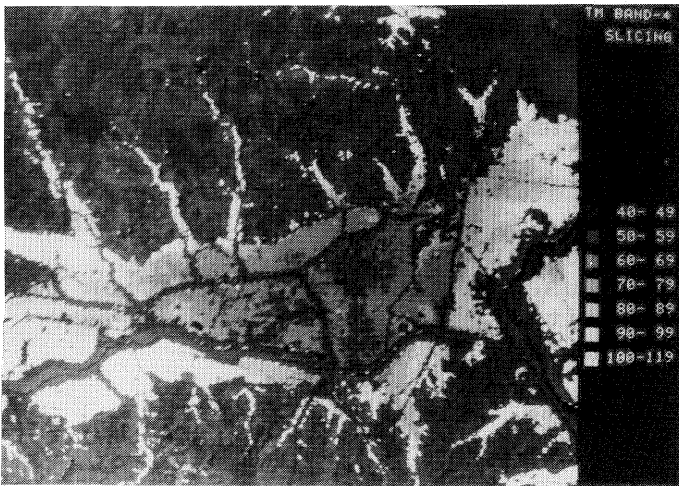


Photo 3
Level sliced picture
of TM band 4

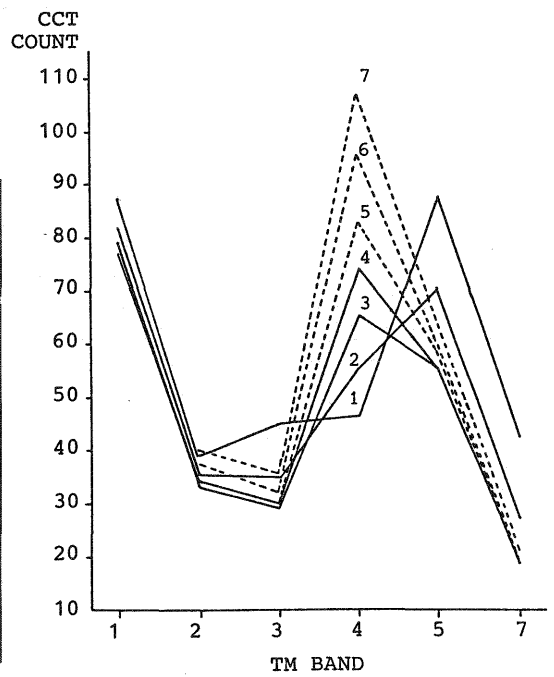


Fig. 3
Spectral signatures
of sampling areas

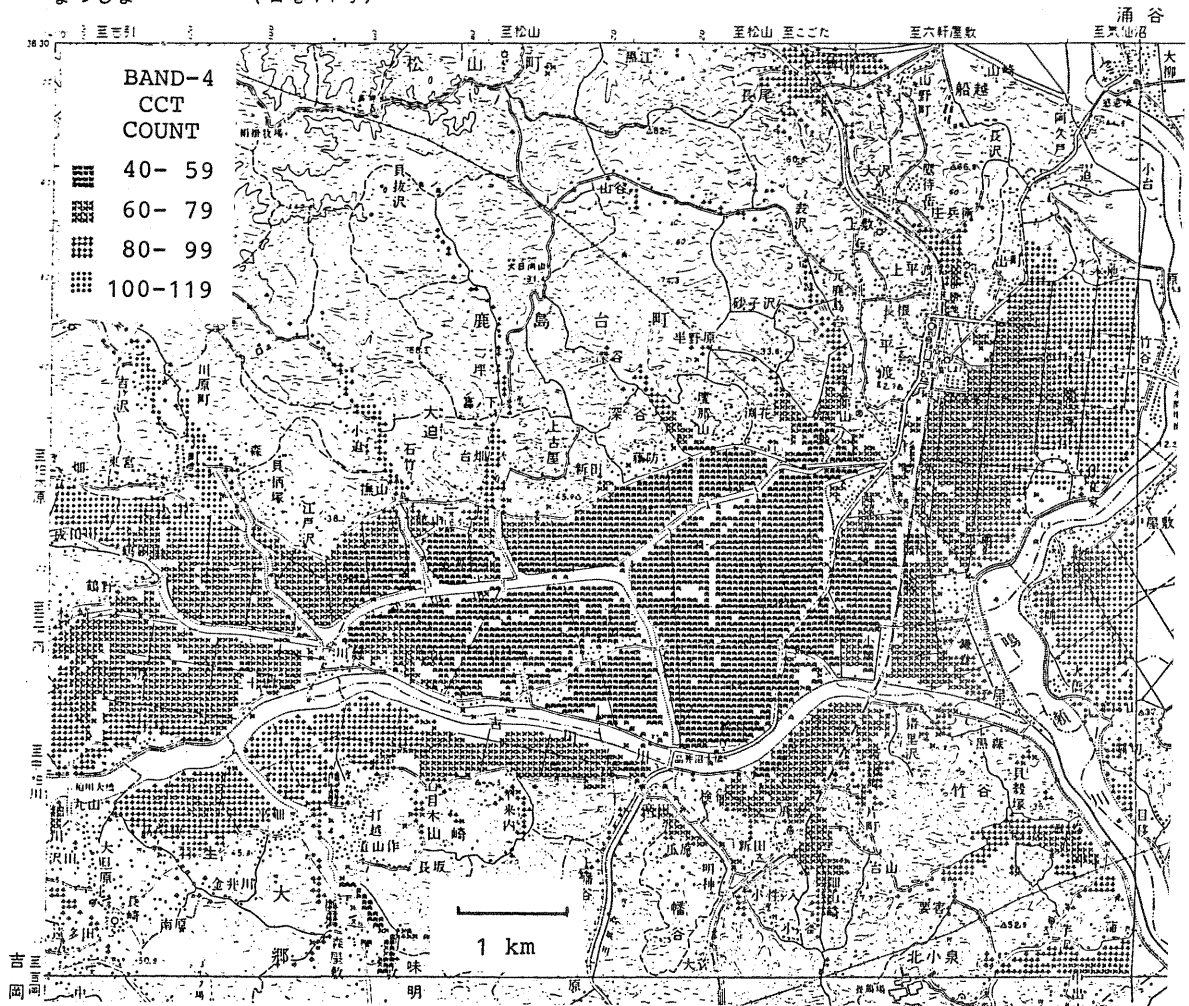


Fig. 4 Regional distribution of the damage on rice-plant detected from TM band 4 by level-slicing

| Region Number | CCT Count | Inundation (Days) | Yield (kg/10a) |
|---------------|-----------|-------------------|----------------|
| 1 | 40-49 | 8- | 0 |
| 2 | 50-59 | 6-7 | 0 |
| 3 | 60-69 | 5 | -100 |
| 4 | 70-79 | 3-4 | -200 |
| 5 | 80-89 | 2 | -300 |
| 6 | 90-99 | 1 | -400 |
| 7 | 100-119 | -1 | -565 |

Table 1 Comparison with the ground survey data

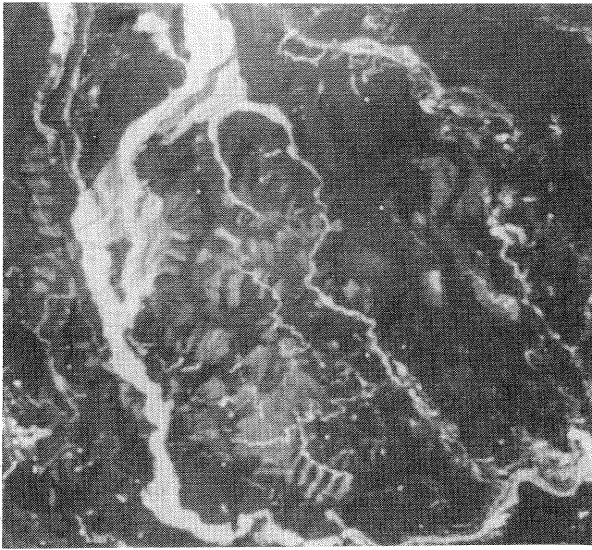


Photo 4
TM image of Band 3

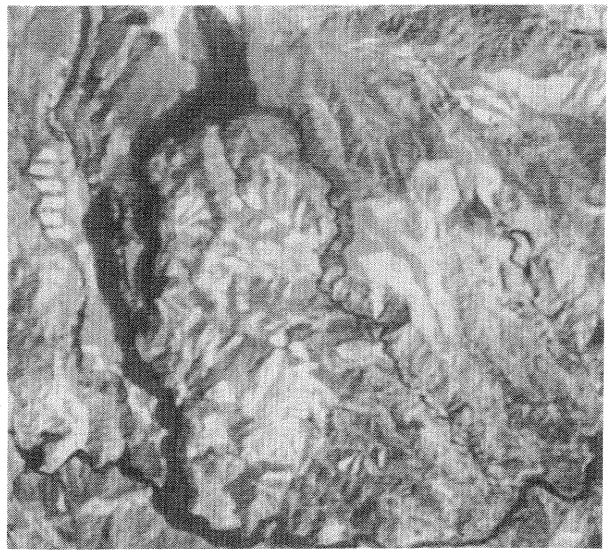


Photo 5
TM image of Band 4

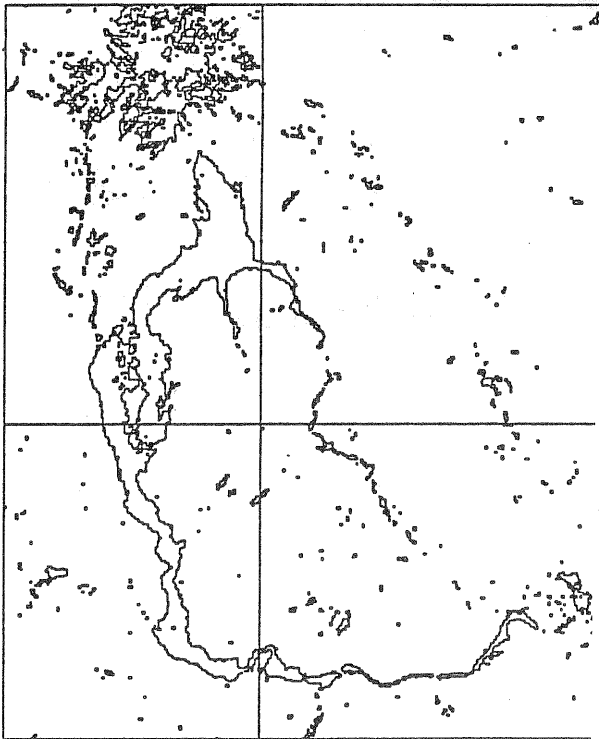


Fig. 5
Boundaries of landslides
detected by the supervised
classification of TM data

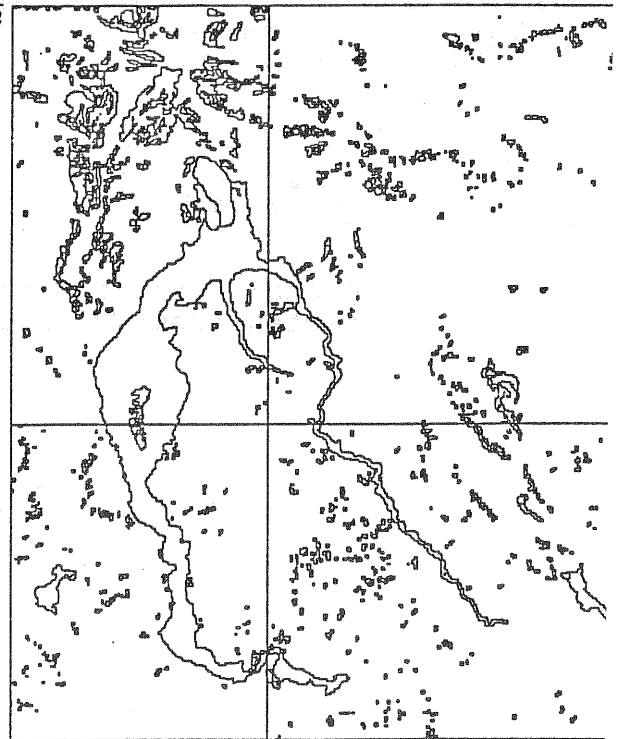


Fig. 6
Boundaries of landslides
interpreted from
aerial photographs

0 3km

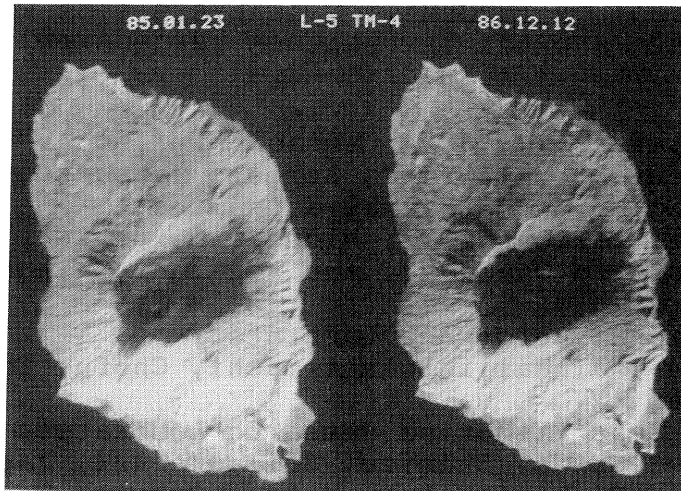


Photo 6 TM image of Band 4
before(left) and after(right)
the eruption

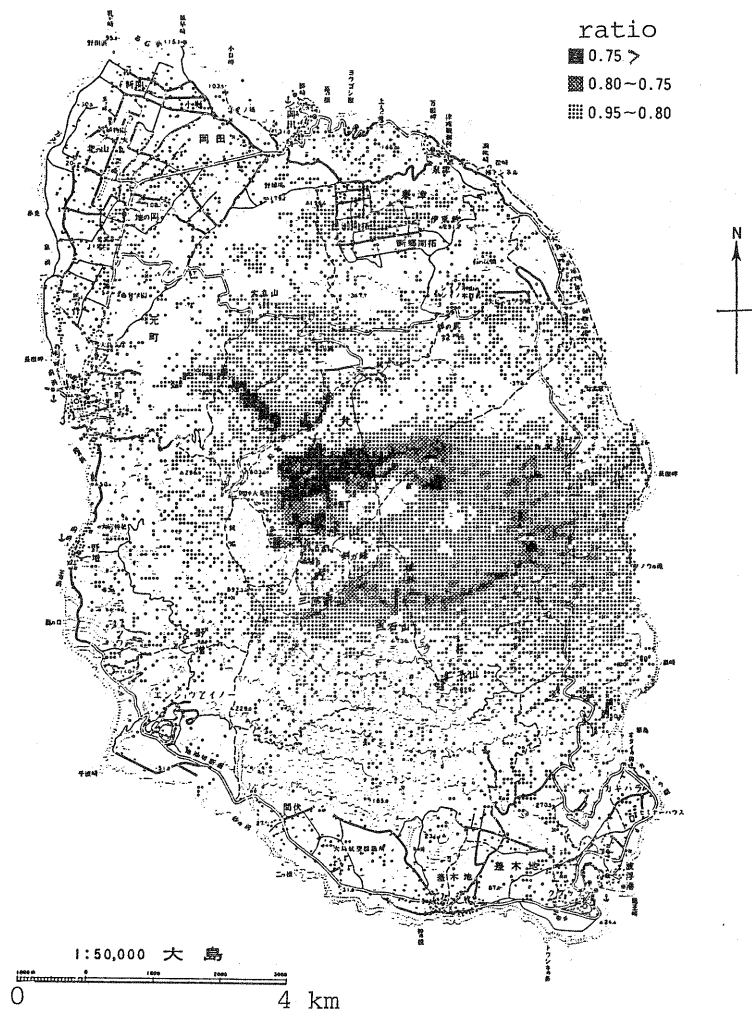


Fig. 7 Regional distribution of volcanic ejecta
detected from the ratio of the two times